Journal Name

Role of charge transfer states into the formation of cyclobutane pyrimidine dimers in DNA

Wook Lee,[a] and Spiridoula Matsika[*b]

Photoinduced charge transfer between neighboring bases plays an important role in DNA. One of its important effects is shown in its ability to affect the photochemical yields of the formation of cyclobutane pyrimidine dimer (CPD) products between adjacent pyrimidine bases. In this work we examine how the energies of charge transfer states depend on the sequences of oligonucleotides by using a hybrid quantum and molecular mechanics (QM/MM) methodology combined with the algebraic diagrammatic construction through second order electronic structure method for excited states. Specifically, we examine 10 sequences with guanine being on the $5'$ or $3'$ position of two pyrimidine bases. The results show that the energies of charge transfer states are affected by the nature of donor acceptor pair, by the distance between them, and by other electrostatic effects created by the surrounding environment.

1   Introduction

Even though DNA is quite photostable, photochemical reactions can occur with low yield.[1,2] The most common photochemical product after absorption of UV radiation by DNA is the formation of cyclobutane pyrimidine dimers (CPD), formed by cycloaddition [2 + 2] between the C5-C6 double bonds of two pyrimidines.[1] Although all pyrimidine dimers can form these products, it has been determined that Thymine-Thymine (TT) is the most photoreactive sequence followed by Thymine-Cytosine (TC), whereas lower amounts of damage are produced at Cytosine-Thymine (CT) and Cytosine-Cytosine (CC) sites.[3]

The quantum yield of thymine dimer formation is significantly influenced by adjacent bases, and a correlation between the degree of quenching and the oxidation potential of the flanking base had been observed experimentally.[4–7] A theoretical explanation for these observations was provided by our previous work, which demonstrated that electron transfer from the flanking base to thymine, facilitated by a charge transfer state between these two bases, can provide a decay pathway for the population to escape from dimer formation, which eventually leads to the formation of an exciplex.[8]

In addition to the quenching effect, it was also found that in some cases the charge transfer states can have an opposite effect and actually enhance the reactivity. This pathway involves the for-

mation of an exciplex which facilitates intersystem crossings. In this case CPD is formed through triplet states.[9] This mechanism is not expected to be widely operative. Its relevance depends on the characteristics of the exciplex formed through the charge transfer states. Specifically, the exciplex should lead to diradicals with two radical centers separated by relatively large distances, and as a result, the singlet and triplet states are degenerate facilitating intersystem crossing. Formation of CPD through this mechanism occurs through sequential steps and its existence is supported by the experimental detection of triplet intermediates.[10]

Overall, the importance of electron transfer in the reactivity of oligonucleotides has been highlighted in these previous studies. In the singlet mechanism charge transfer states quench CPD formation while in a triplet mechanism they enhance it. Examining how sequence affects the charge transfer states is crucial in order to understand reactivity, and this is the scope of the current work. We will only examine guanine as a flanking base because it has the lowest oxidation potential among the four standard nucleic acid bases, allowing easy access to the charge transfer states, and was shown to have the greatest quenching effect. We will focus on three effects: Initially, we will examine how guanine affects the formation of CPD in the different pyrimidine dimers, TT, CT, TC, and CC. Subsequently, we will examine the effect of placing guanine on the $5'$ position or the $3'$ position in the sequence. Finally, the effect of methylation of cytosine on charge transfer states will be examined.

^{a} Department of Chemistry, Pohang University of Science and Technology (POSTECH) , Pohang 37673, Korea.
^{b} Department of Chemistry, Temple University, Philadelphia, PA 19122, USA. Tel: +1 215 204 7703; E-mail: smatsika@temple.edu

2 Computational details

A total of 10 model systems, where the core sequences were inserted in the middle of duplex DNA (18-mer for the TTG sequence and 17-mer for the rest), were created (see Figure 1). The initial structures of duplex DNA for each model system were built using NAB module[11] in AMBER Tools Ver. 1.5. The AMBER ff99 parameter set[12] with bsc0 corrections[13] was used for standard nucleic acids and the general AMBER force field (GAFF) parameter set[14] was used for 5-methylcytosine residue. The atomic partial charges for 5-methylcytosine were fitted using the restrained electrostatic potential (RESP) method.[15] Here, the required potentials were computed using HF/6-31G* on the structure optimized with B3LYP/6-31G*, and these calculations were done using Gaussian03.[16] The initial structures were then solvated in a truncated octahedral box filled with TIP3P water molecules[17] in which the minimum distance between any atom in solute and the edge of the box is 8 Å. The system was neutralized by adding Na^+ counter ions. All model systems were minimized for 500 steps to avoid any possible steric crashes, and then the temperature was gradually increased from 0 to 300K with positional restraints on the solute. After reaching 300K, the restraints were gradually removed, and equilibration was carried out for 1 ns followed by 2 ns of productive MD run. All MD simulations were performed using the sander module of AMBER 11.[18] The temperature was controlled using the Langevin thermostat, and the pressure was kept at 1 bar with Berendsen's weak-coupling algorithm.[19] The SHAKE algorithm was applied on all bonds including hydrogen atoms,[20] and a time step of 2 fs was used. Periodic boundary conditions were employed, and the cut-off distance of 8 Å was adopted for non-bonded interactions. For long-range electrostatic interactions, the particle mesh Ewald summation method was used.[21]

For QM/MM calculations, the Chemshell suite[22] was used to provide an interface between QM and MM calculations. The Turbomole program package[23] and DL-POLY code[24] were used for QM and MM calculations, respectively. The link atom scheme was employed at the boundary of QM and MM,[22] and the charge shift scheme was applied to avoid overpolarization.[25] A total of 20 snapshots separated by an equal interval were extracted from 2 ns of MD simulation trajectory for each model system, and water molecules farther than 25 Å away from the central base of duplex DNA in all snapshots were removed for computational efficiency. All snapshots then underwent ground state energy minimization with BLYP/TZVPP[26-29] in conjunction with Grimme's dispersion correction[30] before vertical excitation energy calculations, and all residues farther than 10 Å away from the central base were frozen during these minimizations. Since we are focusing on only the charge transfer state and also dealing with many sequences, the QM region includes only two bases, namely, the flanking guanine and its neighboring pyrimidine, for computational efficiency. Comparisons of the current results with the previous study where we included three bases[8] shows that the difference of the average of charge transfer states is about 0.1 eV, and it should not affect any of our conclusions.

Vertical excitation energies were computed using the alge-
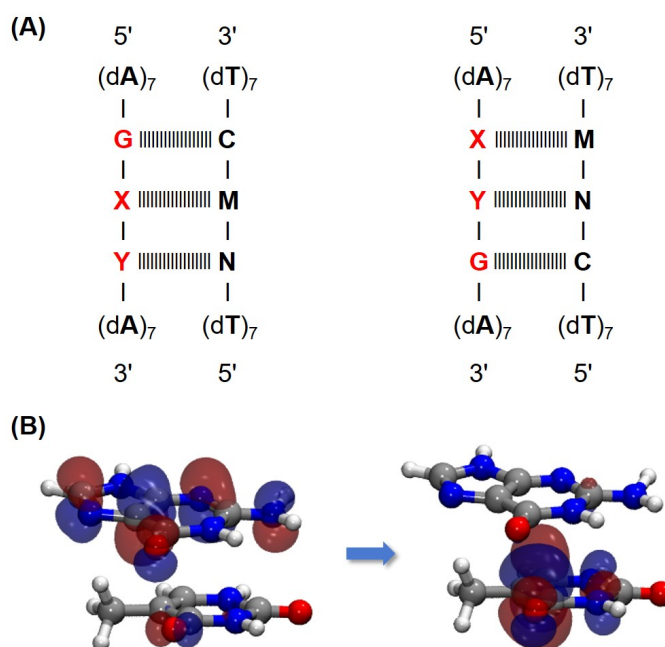
Fig. 1 Schematic representation of the duplex DNA model systems examined in this work (A) and an exemplary natural transition orbital of a charge transfer state (B). X and Y shown in (A) are the sequences of interest and M, N are their complementary bases, respectively.

braic diagrammatic construction through second order (ADC(2)) method[31,32] with the def2-SVP basis set.[29] VMD[33] was used to visualize natural transition orbitals[34] and measure distances.

In order to generate the potential energy profile of TC, geometry optimizations were performed with the constraint on the distance d between the middle point of the C5-C6 double bonds of the two pyrimidine bases. After the constrained geometry optimizations with dispersion corrected BLYP/TZVPP at each point, vertical excitation energy calculations with ADC(2)/def2-SVP were followed. Further constrained optimization on the ground state leads to the CPD product. The potential energy profile of TT was adopted from our previous study[8] and redrawn.

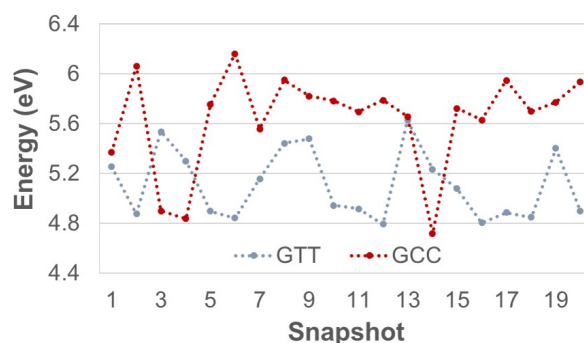## 3 Results and Discussion

3.1 Mechanism for CPD Formation

This work is motivated by previous findings that charge transfer states play an important role in the quantum yields of the photochemical formation of CPD. In previous work we examined the formation of CPD in TT sequences.[8] It was shown that the lower energy exciton state formed from the $\pi\pi^*$ state in thymine is responsible for the formation of CPD. The reactive state becomes obvious when we plot the excited states as a function of the distance between the double bonds in thymine (see Figure 2A). While all other states are destabilized when the two thymine bases approach each other, one of the exciton states remains stable. In previous work we proved that optimization along that surface eventually leads to the CPD product (depicted in Figure 2A).). Therefore, we will refer to this state as dimer precursor (DP) state and the other state from excitonic coupling as DP-2 state. In addition, two $n\pi^*$ excitations of each constituting
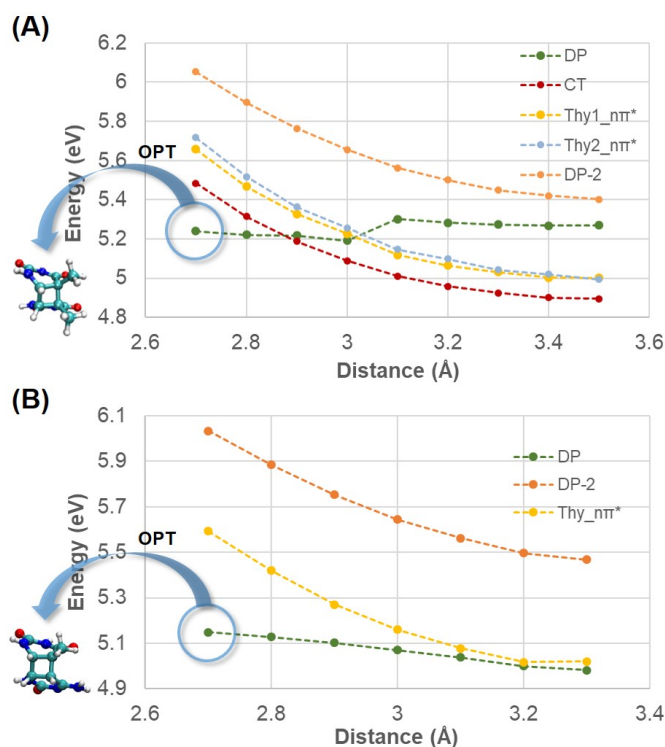
Fig. 2 Potential energy profiles of (A) TT and (B) TC along the distance d between the two pyrimidine bases.

Fig. 3 Energy of charge transfer states for GTT and GCC for 20 snapshots.

thymine are denoted as Thy1_$n\pi^*$ and Thy2_$n\pi^*$, and the charge transfer state is denoted as CT in Figure 2A). In order to check the generality of these arguments we calculated similar potential energy profiles for the TC dimer. Figure 2B shows the plot for the TC dimer where we observe the same behavior for the reactive state as we had seen in TT, i.e. the lower exciton state is stable with respect to the distance d between the two pyrimidine bases. This validates our argument that the photochemistry between two pyrimidine bases should proceed through similar pathways, and the importance we observed between the interplay of charge transfer and DP states in TT holds for the other dimers. Several theoretical studies examining the mechanism for CPD formation have been published, ranging from studies of gas phase bases to more complicated oligonucleotides.[35–46] The nature of the state responsible for CPD formation has been debated in the literature. While many studies agree with our conclusions that the lowest exciton is the reactive state[45,46] an alternative explanation has been given, namely that a doubly excited state is responsible.[44] Doubly excited states are too high in energy to be populated directly by absorption, however. Furthermore, when the distance between the two pyrimidine bases becomes short the pathway is the same regardless of the initial state. Doubly excited states cannot be described by single reference methods, such as ADC(2), but a study employing both single and multireference methods agrees that the DP state is responsible for the photoproduct.[45]

Based on our previous work, it is expected that the lower the energy of the charge transfer states the stronger the quenching effect will be. For instance, the quenching will take place if the excited population transfers from DP to CT through nonadiabatic transitions around the area of maximum coupling, which is shown in our 1-dimensional picture in Figure 2A to be around 2.9 Å where the two states cross. Therefore, after we establish that the DP state should be similar in the different pyrimidine sequences (please note that this work is not examining any inherent differences in the reactivity of the pyrimidine bases.), we mainly focus on the energy of charge transfer states, and systematically examine the factors affecting the energetic location of the charge transfer states in the context of various sequences. To this end, we create model systems where the sequence of interest inserted in the middle of duplex DNA (Figure 1(A)) and compute the excitation energies of the charge transfer state in each model system. The sequence of interest is comprised of two pyrimidine bases and one flanking guanine at either 5′ or 3′ side. Figure 1(B) shows the natural transition orbitals describing a charge transfer state and shows that electron density is shifted from the flanking guanine to an adjacent pyrimidine base.

3.2 Factors Affecting the Energy of Charge Transfer States
3.2.1 Effect of sequence: GTT, GTC, GCT, GCC

We first examine the four pyrimidine dimers, TT, CT, TC, and CC with guanine placed at the 5′ position. The difference in reactivity between TT and CC has been studied experimentally before for isolated dimers.[39] The intrinsic differences in the reactivity of the pyrimidines are not examined in this work, where we only focus on the charge transfer states between guanine and the pyrimidine next to it.

Figure 3 shows the energy of charge transfer states for all 20 snapshots for two of the systems we compare in this section (GTT and GCC) as a representative example of how the charge transfer states fluctuate based on the fluctuations of the environment. The charge transfer states depend on the environment and there are strong variations in all cases. The standard deviation is 0.2-0.4 eV for all systems studied in this work. From now on we will use the average energies produced from these snapshots since they represent a more compact way to analyze the results.

The average energies of charge transfer states for all systems are shown in Figure 4A. The energy of the charge transfer states change significantly for the four sequences, GTT, GTC, GCT, GCC.

The charge transfer states in GTT have the lowest energy, with an average of 5.1 eV, followed by GTC with an average of 5.4 eV. On the other hand, GCT and GCC both have charge transfer states with average energies at 5.6 eV (5.6335 and 5.6379 eV, respectively). This pattern shows that when guanine is π-stacked with thymine the charge transfer states are stabilized compared to when guanine is π-stacked with cytosine. The main effect is caused by the first neighbors, i.e. whether guanine is next to thymine or cytosine. There is however a small secondary effect by the second neighboring base. This is evident when comparing GTT to GTC or GCC to GCT. For GTT and GTC for example, guanine is on the 5′ position of thymine, but the difference is the base next to thymine, which is either thymine or cytosine. This secondary effect is < 0.3 eV, compared to the main effect which is as large as 0.6 eV.

These results indicate that quenching of the reactivity to form CPD should be more important for GTT and GTC but less important for GCC and GCT.

### 3.2.2 Effect of guanine being on the 5′ vs. 3′ position

We next examine the effect of placing guanine on the 5′ vs. 3′ position. Figure 4A shows the average energies of the charge transfer states for five pairs of sequences. In each pair guanine has been placed either on the 5′ or the 3′ position of reactive pyrimidine dimer. In the first two pairs (GTT, TTG, GTC, and CTG), the neighboring pyrimidine next to guanine is always thymine, while it is cytosine in the next two pairs (GCT, TCG, GCC, and CCG). In the last pair, methylated cytosine is adjacent to guanine. In the two pairs in the middle (GTC, CTG, GCT, and TCG), the two pyrimidines are asymmetric. Since we have observed that the effect of guanine is very different in T compared to C, in order to exclude the effect of different bases and focus only on the 5′ vs. 3′ effect, we compare GTC(GCT) with CTG(TCG), where in both cases G is adjacent to T(C). For similar reasons the fifth pair involves the sequences GmCT and TmCG.

In all five pairs, it is clearly shown that the energy of the charge transfer states is stabilized when guanine is on the 5′ position compared to the 3′ position. The effect is not equivalently strong in all cases. In GmCT the effect is the strongest with the charge transfer state blueshifted by 0.64 eV moving from the 5′ to the 3′ position, and the effect is getting weaker in the order of GTT, GTC, GCC, and GCT.

In this case, we can again relate the energy of charge transfer states to the quenching of CPD formation. Our results indicate that guanine on the 5′ position is a stronger quencher of reactivity compared to guanine on the 3′ position. The change in the quenching behavior of guanine for TT based on the position (GTT vs. TTG) has been indeed observed experimentally in single strands and hairpins[6] and in double strands.[7]

3.2.3 Effect of methylation

Finally, we examine the effect of methylation. It has been observed that methylation has a pronounced effect on the CPD formation. Comparisons of TCG and TmCG have shown that the yield for dimerization increases considerably when cytosine is methylated.[5] In our previous study we found that the presence
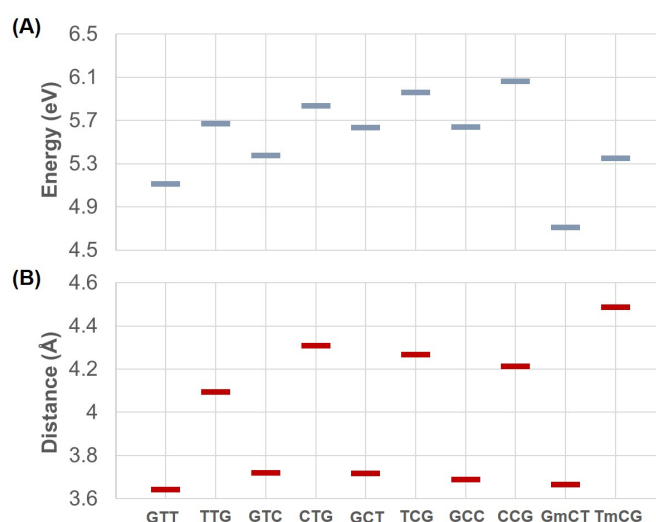
Fig. 4 (A) Average charge transfer energies obtained from 20 snapshots and (B) average distances between two bases involved in charge transfer obtained from 200 snapshots for all sequences

of charge transfer states may be responsible for this.[9] Here we explore further the charge transfer states of sequences with cytosine and methylated cytosine. Specifically we compare two pairs of systems, GmCT vs. GCT and T5mCG vs. TCG. Figure 5(A) shows the average energies of charge transfer states for GmCT, GCT and TmCG vs. TCG. It is obvious that methylation affects the charge transfer states considerably. When cytosine is methylated in GCT the energy of the charge transfer state is stabilized by 0.9 eV, while methylation of TCG leads to a stabilization of 0.6 eV.

3.3 Reasons for Changes in Charge Transfer Energies

The main reasons that can affect the energy of charge transfer states are either intrinsic properties such as difference in the reduction/oxidation potential between the two neighboring bases, or environmental effects such as conformational restriction exerted by helical structure of DNA or electrostatic interactions with surroundings. We examine how these effects have determined the energies of charge transfer states observed in this work.

3.3.1 Redox potentials of bases involved

In our previous work we examined the effect of different flanking bases, guanine, adenine, and cytosine, where the neighboring pyrimidine was always thymine. The redox properties of these bases are quite different, and it was shown that the oxidation potential of flanking bases correlates with the energy level of the charge transfer state, thereby determining whether the charge transfer state intersects with the state that can lead to dimer formation. In the current work the flanking base is always guanine but the pyrimidine base can be either thymine or cytosine, and we observed that there is a big effect on the charge transfer states. It turns out that this effect is also correlated with the energies of charge transfer states. The reduction potentials of bases, shown in Table 1, indicate that thymine is the easiest to reduce.[47] The reduction potential of thymine compared to cytosine indicates that
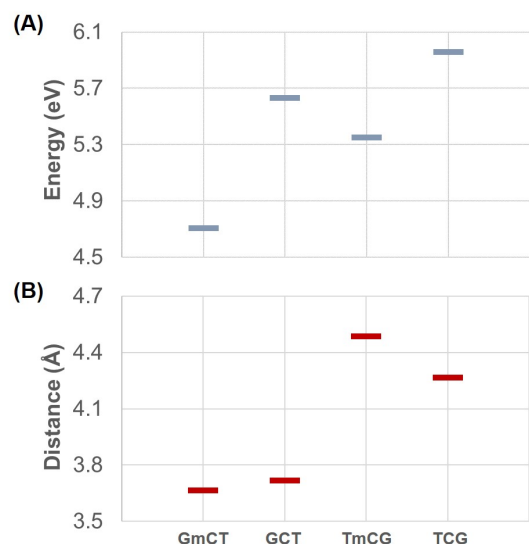
Fig. 5 (A) Average charge transfer energies obtained from 20 snapshots and (B) average distances between two bases involved in charge transfer obtained from 200 snapshots for methylated (GmCT, TmCG) and non-methylated sequences (GCT, TCG).

	Ered/V	Ered/V exp
Guanine	-2.97	<-2.76
Cytosine	-2.36	-2.35
Thymine	-2.31	-2.18
5-Methyl-Cytosine	-2.40	

Table 1 One-Electron Reduction Potentials for DNA Bases, (V vs. NHE) Calculated at M06-2X/6-31++G(d,p) level, taken from Ref. [48]. Experimental values taken from Ref. [49].

reduction of thymine is more favorable than cytosine. Thus there is a stronger driving force for electron transfer from guanine to thymine. This explains the energies of charge transfer states that we see in our calculations. However, this cannot explain the case of methylated cytosine because its reduction potential is more negative than cytosine and thymine, and it should not be reduced as readily. We will return to this issue later.

3.3.2 Conformational restriction by the helix structure of DNA

Besides the redox potentials mentioned above, another factor that affects the energy of the charge transfer states in general is the effects from the environment, which can be divided into electrostatic interactions and conformational restriction. In the case of the positional effect of a flanking guanine at 5′ or 3′ side on charge transfer state energies, the difference must originate from the environment since the constituting bases are identical. In order to probe the reason of this positional effect, we investigated two pairs of sequences, namely, GTT, TTG, GCC and CCG. We chose snapshots from each sequence whose charge transfer energy is close to the average charge transfer energy and removed the MM environments to perform gas phase QM calculations with the constituting bases involved in CT. The results (Table 2) show that the charge transfer energy difference depending on the posi-
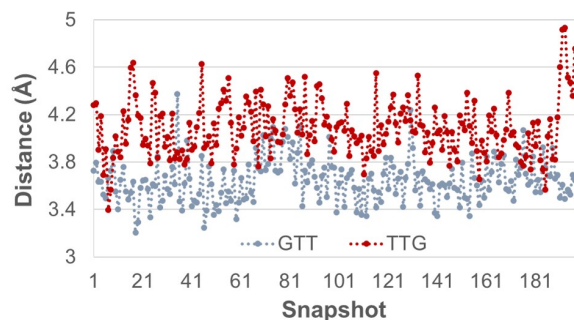
Fig. 6 Distance between the geometric centers of two bases.

tion of a flanking guanine is maintained even after removing the MM environments, indicating that the difference is not attributed to the electrostatic interactions with surroundings. Therefore, the only reason left is conformational restriction exerted by helical structure of DNA. The simplest parameter that can significantly affect the charge transfer state energy is the distance between donor and acceptor, so we collected the distances between the geometric centers of two bases involved in charge transfer from MD trajectories for all sequences. Averages of the distances from 200 snapshots are shown in Figure 4(B), and the average distance between the centers of guanine and pyrimidine is 3.6-3.7 Å when guanine is on the 5′ position, while the average distance is 4.1 -4.5 Å when guanine is on the 3′ position. The difference in the charge transfer energies due to the position of guanine at 5′ or 3′ side (Figure 4(A)) exhibits clear correlation with the difference in the distances (Figure 4(B)), indicating that the charge transfer energy difference resulting from the position of guanine at 5′ or 3′ side is attributed to the distance between the bases involved in CT.

Figure 6 shows the actual data used to produce the averages for GTT and TTG. It is clear that there is a great variation in the distances, but the distances in TTG are almost always higher than those of GTT. Thus, the average is a very good indicator of the behavior.

3.3.3 Electrostatic interactions with surroundings

The charge transfer energy difference between sequences including methylated cytosine and its non-methylated counterpart should also originate from the environmental effects since the redox potential of methylated cytosine is comparable to that of non-methylated one (Table 2). However, the cause of this charge transfer energy difference is not due to the difference in the distances between the two bases involved in charge transfer, since the average distance observed in TCG is shorter than that of TmCG while the charge transfer energy of TmCG is lower than that of TCG (Figure 5(B)). In the case of GmCT, whose charge transfer energy is much lower than that of GCT, the distance is shorter than that of GCT, but the difference is very small (0.05 Å). We also compared the distance between methylated cytosine and a neighboring thymine to that of the non-methylated sequence, but the distance differences were negligible. Therefore, no correlation is observed between the charge transfer energies and distances in this case, so we conclude that the conformational restric-

	QM/MM	QM
GTT	5.158	5.414
TTG	5.675	6.142
$\Delta E_{TTG-GTT}$	0.517	0.728
GCC	5.629	5.271
CCG	6.082	5.854
$\Delta E_{CCG-GCC}$	0.453	0.583
GmCT	4.7	5.731
GCT	5.649	5.231
$\Delta E_{GCT-GmCT}$	0.949	-0.5
TmCG	5.262	6.103
TCG	5.942	5.803
$\Delta E_{TCG-TmCG}$	0.68	-0.3

Table 2 Energies of charge transfer states (in eV) for a representative snapshot calculated using the whole model system (QM and MM) and only the QM region. The energy difference Δ between the two previously listed sequences is also shown.

tion exerted by helical structure is not the reason of the difference in charge transfer energies here.

As a next step, we performed gas phase calculations without the MM environment to evaluate the effect of electrostatic interactions with the surroundings (Table 2). Interestingly, the energetic order of charge transfer state between the methylated sequence and its counterpart becomes reversed after turning off the charges from the environment, and the charge transfer energy of methylated sequence is now higher than that of the non-methylated counterpart. This is clearly opposite from the case observed in the charge transfer energy difference caused by the position of a flanking guanine. The bulky methyl group of cytosine seems to distort the surrounding structures, resulting in differences in structures from those of non-methylated one, and it is quite interesting that this distortion leads to the rearrangement of surrounding charges in a way to stabilize the charge transfer energies.

4 Conclusions

We used QM/MM calculations to examine how the energies of charge transfer states change for 10 different sequences that include a pair of pyrimidine dimers which can be photo-dimerized to form CPD. All sequences include guanine as the flanking base. In the first tetrad (GTT, GTC, GCT, GCC) we examined how the different pyrimidines can affect charge transfer states, and we found that when guanine is next to thymine the charge transfer states are low in energy while they are destabilized when guanine is neighboring cytosine. The secondary base has a much smaller effect. The second effect we examined was how placement of guanine at the 5′ vs. 3′ side changes the charge transfer states, and we found that guanine at the 3′ position destabilizes the charge transfer states. Finally, methylation of cytosine was found to lead to extra stabilization of charge transfer states. Overall, this work shows that the energies of charge transfer states are affected by (i) the nature of donor acceptor pair, (ii) the distance between them and (iii) other environmental effects created by the surrounding environment.

5 Acknowledgement

References

1 J. Cadet, S. Mouret, J.-L. Ravanat and T. Douki, *Photochemistry and Photobiology*, 2012, **88**, 1048–1065.

2 J. Cadet, A. Grand and T. Douki, *Top. Curr. Chem.*, 2015, **356**, 249.

3 T. Douki and J. Cadet, *Biochemistry*, 2001, **40**, 2495–2501.

4 M. R. Holman, T. Ito and S. E. Rokita, *J. Am. Chem. Soc.*, 2007, **129**, 6–7.

5 V. J. Cannistraro and J.-S. Taylor, *J. Mol. Biol.*, 2009, **392**, 1145–1157.

6 Z. Pan, M. Hariharan, J. D. Arkin, A. S. Jalilov, M. McCullagh, G. C. Schatz and F. D. Lewis, *J. Am. Chem. Soc.*, 2011, **133**, 20793–20798.

7 Y. K. Law, R. A. Forties, X. Liu, M. G. Poirier and B. Kohler, *Photochem. Photobiol. Sci.*, 2013, **12**, 1431.

8 W. Lee and S. Matsika, *Phys.Chem.Chem.Phys.*, 2015, **17**, 9927–9935.

9 W. Lee and S. Matsika, *ChemPhysChem.*, 2018, **19**, 1568 – 1571.

10 B. M. Pilles, D. B. Bucher, L. Liu, P. Clivio, P. Gilch, W. Zinth and W. J. Schreier, *J. Phys. Chem. Lett.*, 2014, **5**, 1616–1622.

11 T. Macke and D. A. Case, in *Modeling Unusual Nucleic Acid Structures. In Molecular Modeling of Nucleic Acids*, ed. N. B. Leontes and J. J. SantaLucia, Washington, DC: American Chemical Society, 1998, ch. 24, pp. 379–393.

12 J. Wang, P. Cieplak and P. Kollman, *J. Comput. Chem.*, 2000, **21**, 1049–1074.

13 A. Peréz, I. Marchán, D. Svozil, T. E. I. I. I. Cheatham, C. A. Laughton and M. Orozco, *Biophys. J.*, 2007, **92**, 3817–3829.

14 J. Wang, R. M. Wolf, J. W. Caldwell, P. Kollman and D. A. Case, *J. Comput. Chem.*, 2004, **25**, 1157–1174.

15 C. I. Bayly, P. Cieplak, W. Cornell and P. Kollman, *J. Phys. Chem.*, 1993, **97**, 10269–10280.

16 M. J. Frisch, G. W. Trucks, H. B. Schlegel, G. E. Scuseria, M. A. Robb, J. R. Cheeseman, J. A. Montgomery Jr., T. Vreven, K. N. Kudin, J. C. Burant, J. M. Millam, S. S. Iyengar, J. Tomasi, V. Barone, B. Mennucci, M. Cossi, G. Scalmani, N. Rega, G. A. Petersson, H. Nakatsuji, M. Hada, M. Ehara, K. Toyota, R. Fukuda, J. Hasegawa, M. Ishida, T. Nakajima, Y. Honda, O. Kitao, H. Nakai, M. Klene, X. Li, J. E. Knox, H. P. Hratchian, J. B. Cross, V. Bakken, C. Adamo, J. Jaramillo, R. Gomperts, R. E. Stratmann, O. Yazyev, A. J. Austin, R. Cammi, C. Pomelli, J. W. Ochterski, P. Y. Ayala, K. Morokuma, G. A. Voth, P. Salvador, J. J. Dannenberg, V. G. Zakrzewski, S. Dapprich, A. D. Daniels, M. C. Strain, O. Farkas, D. K. Malick, A. D. Rabuck,

K. Raghavachari, J. B. Foresman, J. V. Ortiz, Q. Cui, A. G. Baboul, S. Clifford, J. Cioslowski, B. B. Stefanov, G. Liu, A. Liashenko, P. Piskorz, I. Komaromi, R. L. Martin, D. J. Fox, T. Keith, M. A. Al-Laham, C. Y. Peng, A. Nanayakkara, M. Challacombe, P. M. W. Gill, B. Johnson, W. Chen, M. W. Wong, C. Gonzalez and J. A. Pople, *Gaussian 03, Revision C.02*, 2004.

17 W. Jorgensen, J. Chandrasekhar, J. Madura and M. Klein, *J. Chem. Phys.*, 1983, **79**, 926–935.

18 D. A. Case, T. A. Darden, T. E. Cheatham III, C. L. Simmerling, J. Wang, R. E. Duke, R. Luo, R. C. Walker, W. Zhang, K. M. Merz, B. Roberts, B. Wang, S. Hayik, A. Roitberg, G. Seabra, I. Kolossvry, K. F. Wong, F. Paesani, J. Vanicek, J. Liu, X. Wu, S. R. Brozell, T. Steinbrecher, H. Gohlke, Q. Cai, X. Ye, M.-J. Hsieh, G. Cui, D. R. Roe, D. H. Mathews, M. G. Seetin, C. Sagui, V. Babin, T. Luchko, S. Gusarov, A. Kovalenko and P. A. Kollman, *Amber 11, (2010) University of California, San Francisco.*, University of California, San Francisco.

19 H. J. C. Berendsen, J. P. M. Postma, W. F. van Gunsteren, A. DiNola and J. R. Haak, *J. Chem. Phys.*, 1984, **81**, 3684–3690.

20 J. P. Ryckaert, G. Ciccotti and H. J. C. Berendsen, *J. Comput. Phys.*, 1977, **23**, 327–341.

21 U. Essmann, L. Perera, M. L. Berkowitz, T. Darden, H. Lee and L. G. Pedersen, *J. Chem. Phys.*, 1995, **103**, 8577.

22 P. Sherwood, A. H. de Vries, M. F. Guest, G. Schreckenback, C. R. A. Catlow, S. A. French, A. A. Sokol, S. T. Bromley, W. Thiel, A. J. Turner, S. Billeter, F. Terstegen, S. Thiel, J. Kendrick, S. C. Rogers, J. Casci, M. Watson, F. King, E. Karlsen, M. Sjovoll, A. Fahmi, A. Schäfer and C. Lennartz, *J. Mol. Struct. (THEOCHEM)*, 2003, **632**, 1–28.

23 *TURBOMOLE V6.5, a development of University of Karlsruhe and Forschungszentrum Karlsruhe GmbH, 1989-2007, TURBOMOLE GmbH, since 2007; available from* http://www.turbomole.com.

24 W. Smith and T. R. Forester, *J. Mol. Graph.*, 1996, **14**, 136–141.

25 P. Sherwood, A. H. de Vries, S. J. Collins, S. P. Greatbanks, N. A. Burton, M. A. Vincent and I. H. Hillier, *Faraday Discuss.*, 1997, **106**, 79–92.

26 A. D. Becke, *Phys. Rev. A*, 1988, **38**, 3098–3100.

27 W. Y. C. Lee and R. G. Parr, *Phys. Rev. B*, 1988, **37**, 785–789.

28 B. Miehlich, A. Savin, H. Stoll and H. Preuss, *Chem. Phys. Lett.*, 1989, **157**, 200–206.

29 F. Weigend and R. Ahlrichs, *Phys Chem Chem Phys*, 2005, **7**, 3297–3305.

30 S. Grimme, *J. Comput. Chem.*, 2006, **27**, 1787–1799.

31 A. B. Trofimov and J. Schirmer, *J. Phys. B At. Mol. Opt. Phys.*, 1995, **28**, 2299.

32 J. H. Starcke, M. Wormit, J. Schirmer and A. Dreuw, *Chem. Phys.*, 2006, **329**, 39–49.

33 W. Humphrey, A. Dalke and K. Schulten, *J. Mol. Graphics*, 1996, **14**, 33–38.

34 R. L. Martin, *J. Chem. Phys.*, 2003, **118**, 4775–4777.

35 B. Durbeej and L. A. Eriksson, *J. Photochem. Photobiol., A*, 2002, **152**, 95–101.

36 R. B. Zhang and L. A. Eriksson, *J. Phys. Chem. B*, 2006, **110**, 7556.

37 M. Boggio-Pasqua, G. Groenhof, L. V. Schäfer, H. Brubmüller and M. A. Robb, *J. Am. Chem. Soc.*, 2007, **129**, 10996–10997.

38 L. Blancafort and A. Migani, *J. Am. Chem. Soc.*, 2007, **129**, 14540–14541.

39 J. J. Serrano-Pérez, I. González-Ramírez, P. B. Coto, M. Merchán and L. Serrano-Andrés, *J. Phys. Chem. Lett.*, 2008, **112**, 14096–14098.

40 T. Climent, I. González-RamŠrez, R. González-Luque, M. Merchán and L. Serrano-Andrés, *J. Phys. Chem. Lett.*, 2010, **1**, 2072–2076.

41 S. Rössle, J. Friedrichs and I. Frank, *ChemPhysChem*, 2010, **11**, 2011 – 2015.

42 M. Barbatti, *ChemPhysChem*, 2014, **15**, 3342–3354.

43 J. I. Mendieta-Moreno, D. G. Trabada, J. Mendieta, J. P. Lewis, P. Gomez-Puertas and J. Ortega, *J. Phys. Chem. Lett.*, 2016, **7**, 4391–4397.

44 C. Rauer, J. J. Nogueira, P. Marquetand and L. González, *J. Am. Chem. Soc.*, 2016, **138**, 15911–15916.

45 I. Conti, L. Martinez-Fernandez, L. Esposito, S. Hofinger, A. Nenov, M. Garavelli and R. Improta, *Chem. Eur. J.*, 2017, **23**, 15177 – 15188.

46 L. Martínez-Fernández and R. Improta, *Photochem. Photobiol. Sci.*, 2018, **17**, 586.

47 C. E. Crespo-Hernandez, D. M. Close, L. Gorb and J. Leszcynski, *J. Phys. Chem. B*, 2007, **111**, 5386–5395.

48 Y. Paukku and G. Hill, *J. Phys. Chem. A*, 2011, **115**, 4804–4810.

49 C. A. M. Seidel, A. Schulz and M. H. M. Sauer, *J. Phys. Chem.*, 1996, **100**, 5541–5553.